



Cite this: *J. Mater. Chem. B*, 2023,  
11, 11024

## Dendronization of chitosan to afford unprecedented thermoresponsiveness and tunable microconfinement

Yi Yao, Xiaoxin Shi, Zihong Zhao, Afang Zhang \* and Wen Li \*<sup>†</sup>

Convenient chemical modification of biomacromolecules to create novel biocompatible functional materials satisfies the current requirements of sustainable chemistry. Dendronization of chitosan with dendritic oligoethylene glycols (OEGs) paves a strategy for the preparation of functional dendronized chitosans (DCSs) with unprecedented thermoresponsive behavior, which inherit biological features from polysaccharides and the topological features from dendritic OEGs. In addition, densely packed dendritic OEG chains around the backbone provide efficient cooperative interactions and form an intriguing confined microenvironment based on the degradable biopolymers. In this perspective, we describe the principle for the preparation of the thermoresponsive DCSs, and focus on the molecular envelop effect from the hydrophobic microconfinement to the encapsulated guest molecules or moieties. Particular attention is put on their capacity to regulate behavior and the functions of the encapsulated guests through thermally-mediated dehydration and collapse of the densely packed dendritic OEGs. We believe that the methodology described here may provide prospects for the fabrication of functional materials from biomacromolecules, especially when used as environmentally friendly nanomaterials or in accurate diagnosis and therapy.

Received 9th August 2023,  
Accepted 2nd November 2023

DOI: 10.1039/d3tb01803b

[rsc.li/materials-b](http://rsc.li/materials-b)

## 1. Introduction

Microconfinement plays a vital role for biomacromolecules to exhibit defined biological functions and behavior.<sup>1,2</sup> Biomacromolecules in cells participated in almost all biochemical transformations through a confined and highly crowded environment.<sup>3,4</sup> It has been revealed that crowding of the biomacromolecules accounts for an important factor affecting the folding, association and mobility of proteins and nucleic acids.<sup>3,5</sup> Through molecular design, microconfinement can be realized through molecular crowding or cooperative interactions between structural segments.<sup>2,6</sup> The most intriguing example includes crown ether invented by Peterson, which can bind metal ions specifically from the aqueous phase through cooperative ionic-dipole interactions between donors (oxygens from crown ethers) and acceptors (metal ions).<sup>2,7</sup> Recently, synthetic crowders, for example, Ficoll,<sup>8</sup> dextran,<sup>9</sup> polyethylene glycol (PEG)<sup>6,10</sup> or even copolymers<sup>11,12</sup> have been used at high concentrations to mimic *in vivo* crowding effects and play the role of exerting excluded volume effects, stabilizing proteins, and promoting protein aggregation.<sup>13</sup> However,

these synthetic (macro) molecules for creating a confined microenvironment are normally not biocompatible and biodegradable, which makes it difficult to use them for bioapplications such as drug prolonged delivery.<sup>2,13–15</sup>

Materials based on modified biomacromolecules have been developed in recent years, including tissue adhesives and sealants, scaffolds, and carriers.<sup>16–19</sup> Native biomacromolecules always have difficulty regarding their solubility in conventional media, especially in water.<sup>20–22</sup> Therefore, chemical modification has proven to be an efficient way to assure them better solubility, and at the same time, to enhance their biofunctions and properties.<sup>23</sup> For instance, PEGylation of biomacromolecules has been used as a standard method to improve their stability, solubility, pharmacodynamics, and processability through covalent and non-covalent linkages based on three major strategies, including “grafting to”, “grafting from”, and “grafting through”.<sup>20,24,25</sup> Nonetheless, the precise selection of reaction sites on biomacromolecules for the attachment of synthetic/natural macromolecules or functional units without compromising their structures and activities remains a primary concern.<sup>16,25–27</sup> Moreover, significant efforts are still required to impart biomaterials with stimulus-response characteristics to modulate their properties responding to external stimuli (such as redox, pH, heat, etc.).<sup>28,29</sup> This may provide a similar condition as they had in crowded microenvironments within

*International Joint Laboratory of Biomimetic and Smart Polymers, School of Materials Science and Engineering, Shanghai University, Nanchen Street 333, Shanghai 200444, China. E-mail: [wli@shu.edu.cn](mailto:wli@shu.edu.cn), [azhang@shu.edu.cn](mailto:azhang@shu.edu.cn)*

the cells, which is beneficial for dramatically expanding the advantages of biomacromolecules, creating value-added derivatives, and realizing their commercialization.<sup>10,30–32</sup>

Chitosan (CS), a classical cationic polysaccharide,<sup>33</sup> has received considerable attention as an excellent biomaterial and been widely applied as a nanoreactor,<sup>34</sup> metal adsorbent,<sup>17</sup> and cell culture matrix<sup>35,36</sup> owing to its characteristic features: (1) abundant renewable polysaccharide, mainly derived from the exoskeleton of crustaceans;<sup>18</sup> (2) high stability relative to proteins and nucleic acids;<sup>33,37</sup> (3) multiple functional groups (hydroxyl and amino groups), which can be chemically modified through various reactions and provide effective chelation.<sup>24</sup> The properties and functions of CS can be enhanced and enriched greatly through chemical modifications.<sup>38–40</sup> Conventional modification methods for enhancing the solubility and processability of CS include carboxymethylation, acetylation and phosphorylation, which usually were carried out under harsh conditions (for example, high temperature or strong acid/alkali) or using organic solvent.<sup>21,29,38,41</sup> Recently, versatile mild and eco-friendly methods (such as amidation and Schiff reaction in aqueous solution) have been reported for functional modification of CSs, to improve their properties and expand their applications.<sup>42,43</sup> There are numerous excellent reviews that describe in detail their modifications.<sup>6,33,38,42,44</sup> Linear polymers are frequently used for modification of CS due to their versatile structures and functionsdesignability.<sup>45,46</sup> However, some challenges still remain; for instance, limited grafting efficiency and long reaction time for reasonable coverage.<sup>42,47</sup> Furthermore, long polymer chains also tend to weaken the inherent biological properties of polysaccharides due to the presence of a large proportion of synthetic polymers in the matrices.<sup>22,25,40,47–50</sup> Therefore, it still remains challenging to develop a convenient methodology for the modification of CS, aiming at improving its properties and functions, and at the same time, retaining or even enriching its bio-related properties.<sup>40,42,51</sup>

Dendritic macromolecules possess a branched architecture and multivalency characteristics, which have privilege in the formation of a confined microenvironment and provide cooperative interactions supplying guests with better shielding and protection effect.<sup>2,12,52–57</sup> They have shown intriguing potentials

for modification of CS to form a novel class of dendronized CSs (DCSs), which excellently integrate both natural properties from CS and imparted functions from the dendritic units.<sup>53,58–60</sup> The synthetic strategies of DCSs have had significant advances recently, but these modified entities are still short of stimuli-responsive properties, which hinders the widespread application of these promising materials.<sup>41,61–63</sup> Notably, modification of biomacromolecules, such as gelatin,<sup>47,48</sup> polypeptide,<sup>64,65</sup> and cyclodextrin,<sup>66,67</sup> with stimuli-responsive dendritic oligoethylene glycols (OEGs) is beneficial, because the convergence of superior properties from natural polymers and stimuli-responsiveness generated a series of new intelligent materials, as in our previous reports.<sup>39,53,68–70</sup> Keeping all these in mind, the synergistic combination of features from dendritic architectures and biofunctions from CS, DCSs carrying dendritic OEGs were developed by our group, which show unprecedented thermoresponsiveness and advantages of tunable encapsulation for guests.<sup>53,58–60</sup> Most importantly, the confined microenvironment with stimulus responsive behavior constructed from biodegradable biopolymers modified by dendritic OEGs was for the first time proposed by our group and used for activity regulation of proteins. In this perspective, we mainly outline synthetic strategies and thermoresponsive behavior of the DCSs, focused on their promising switchable encapsulation and function regulation to guests, together with some introduction to the properties of the DCS-based hydrogels (Fig. 1).

## 2. Synthesis of DCSs: strategies and principles

Dendronization of CS with dendritic OEGs not only improves the water solubility and stability of the polysaccharides, but also affords them characteristic thermoresponsiveness inherited from the dendritic OEGs.<sup>34</sup> As shown in Fig. 2A, DCSs carry dendritic diethylene glycol (**DC<sub>XX</sub>**) and dendritic triethylene glycols (**TC<sub>XX</sub>**) were prepared, where the footnote **XX** represents grafting coverage of the dendrons. The dendritic OEGs have varied OEG chain lengths, affording modified CSs with different hydrophilicity to tune their phase transition temperatures

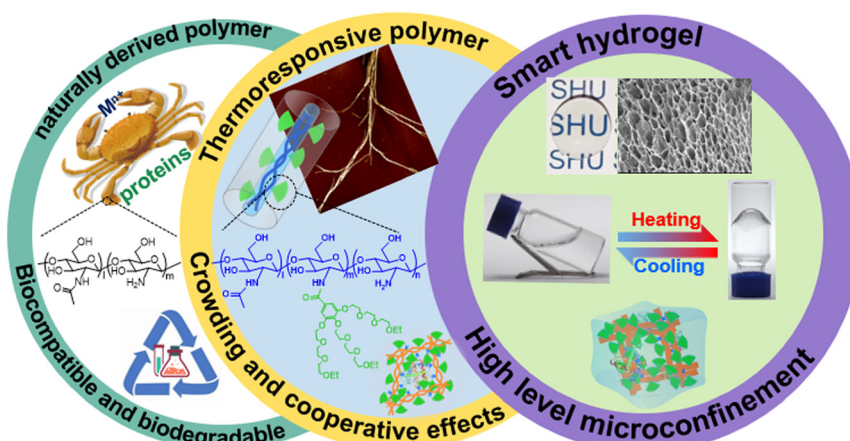
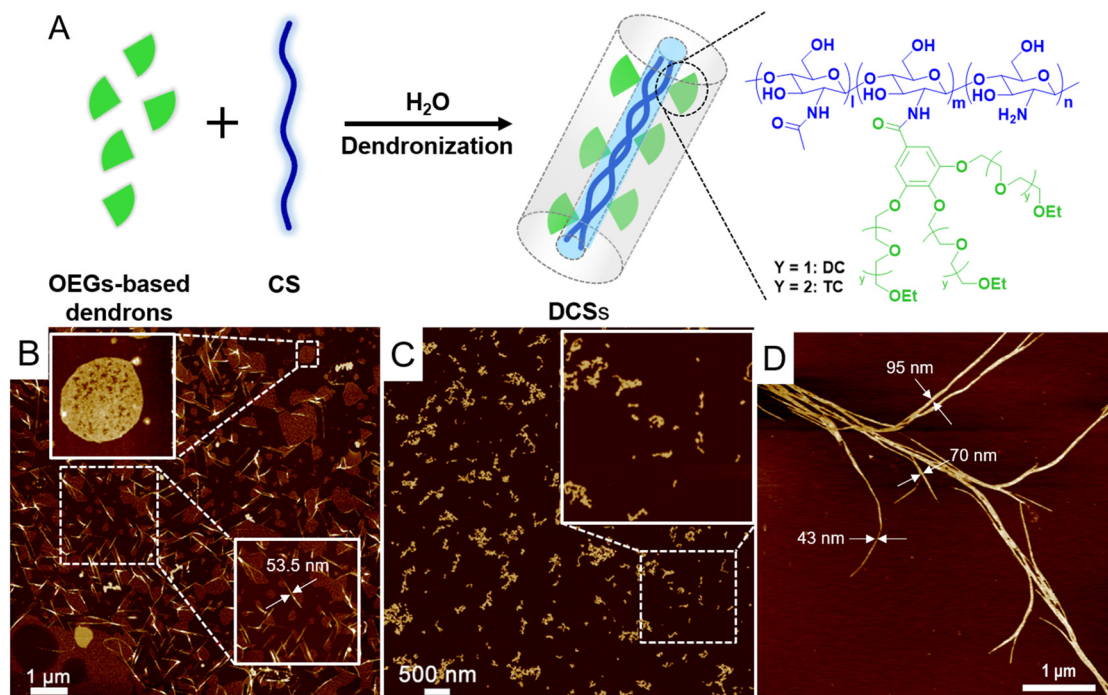


Fig. 1 Illustration of structural, morphology, characteristic, and applications for chitosan, thermoresponsive DCSs, and corresponding smart hydrogels.



**Fig. 2** (A) Cartoon presentation of the synthetic scheme for and molecular structures of DCSs. AFM images from DCSs synthesized from CS with molecular weights of (B) 2 kDa, (C) 150 kDa, and (D) 600 kDa. All samples were prepared on a mica slice from their solutions (0.005 mg mL<sup>-1</sup>). Reproduced from ref. 34, 35 and 72 with permission from American Chemical Society, copyright 2022.

between room temperature and physiological temperature. The dendronization was performed through amidation between carboxyl groups from dendrons and amino groups from CS in aqueous solutions. These DCSs have dendrons wrapped densely around the polymer backbone, rendering them in a wormlike geometry. The densely packed OEG chains along the backbone provide remarkable microconfinement on a molecular level, and impart DCSs with intriguing radial amphiphilicity, resulting in the assembly of the polymers to form fibers in aqueous solution with the length and thickness dependent on the molecular weight of chitosan (Fig. 2B–D). This assembly behavior of DCSs in water has been confirmed to contribute to thermally-induced aggregation and gelation of the polymers.<sup>35,71</sup>

### 3. Thermoresponsive behavior of DCSs

DCSs inherited unprecedented thermoresponsive properties from densely packed dendritic OEGs.<sup>34,59,71,72</sup> Both **DC<sub>XX</sub>** and **TC<sub>XX</sub>** exhibited good solubility in aqueous solutions or phosphate buffer (PBS) at 20 °C, and the solutions are clear to visualize the logo, as shown in Fig. 3A. However, their dilute solutions turned into turbid at elevated temperature, indicating characteristic thermoresponsive behavior, and the cloud point temperatures ( $T_{\text{cp}}$ ) are dependent on topological structure, grafting ratio of OEG dendrons, and concentration of DCSs.<sup>71,72</sup> The corresponding concentrated solutions (>0.5 wt%) transformed into gels over the gelation points ( $T_{\text{gel}}$ ). The main results include:

(1) both the  $T_{\text{cp}}$ s and  $T_{\text{gel}}$ s of the DCSs decreased with the increase of dendron coverage (Fig. 3A and B), where the dendron grafting ratios on DCSs were calculated by acid–base titration.<sup>71</sup> (2) **DC<sub>XX</sub>** pendant with short lengths of OEG chains was more hydrophobic, and exhibited lower  $T_{\text{cp}}$  and sharper phase transition with smaller hysteresis compared to the **TC<sub>XX</sub>** with the similar grafting ratios (Fig. 3A and C). (3)  $T_{\text{gel}}$  decreased with increase of the DCS concentration (Fig. 3D). Moreover, through their electrostatic combination with guest molecules, there is hardly any influence on the thermally-induced collapse and aggregation behavior of the DCSs.<sup>34</sup> The above thermoresponsive behavior demonstrates that the periphery of dendrons wrapped around the cylindrical DCSs dominates their apparent amphiphilicity and provided efficient shielding to the chitosan interiors.

### 4. DCSs acting as molecular envelopes

#### 4.1 Switchable encapsulation of metal ions

The complexation between DCSs and metal ions was explored by using  $\text{Ag}^+$  and  $\text{AuCl}_4^-$  as the models under conditions below their  $T_{\text{cp}}$  or during their thermally-induced collapse (Fig. 4A). The maximum binding capacity of DCSs with 40% dendron coverage ( $\text{TC}_{0.4}$ , 22.4  $\mu\text{g mg}^{-1}$ ) to  $\text{Ag}^+$  was close to that of linear OEG-modified CSO ( $\text{LC}_{0.4}$ ) and nearly half of that for the naked chitosan oligosaccharide (CSO, 48.1  $\mu\text{g mg}^{-1}$ ) at 25 °C, but there was no complexation for the case of OEG-based dendronized polymethacrylate **PG1** (Fig. 4B), suggesting that the CS backbones provide the key structural units for ion binding,

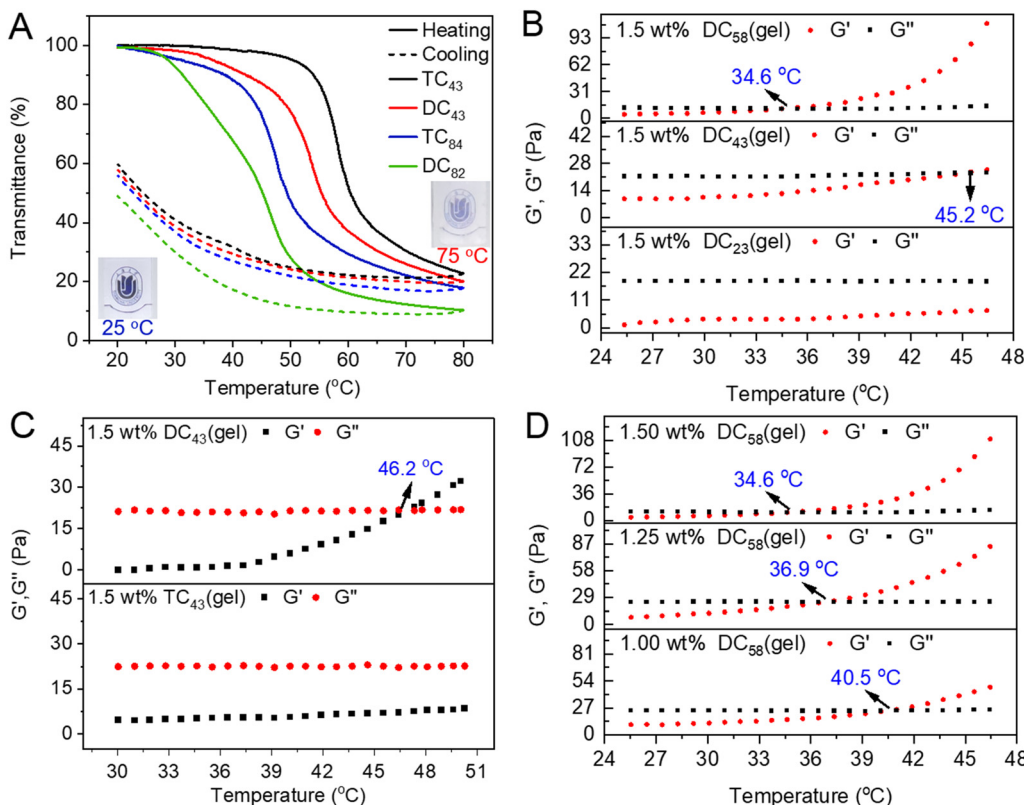


Fig. 3 Thermoresponsive behavior of DCSs. (A) Plots of transmittance vs. temperature for DCSs in PBS. Temperature dependence of the storage modulus  $G'$  and loss modulus  $G''$  of the DCSs and corresponding hydrogels, (B)  $DC_{23}(gel)$ ,  $DC_{43}(gel)$ , and  $DC_{58}(gel)$ , (C)  $DC_{43}(gel)$  and  $TC_{43}(gel)$ , and (D)  $DC_{58}(gel)$  at different concentrations. Reproduced from ref. 71 with permission from American Chemical Society, copyright 2022.

mainly due to the interaction between amino or hydroxyl groups to metal ions. Moreover, compared to others,  $Ag^+$  embedded in DCSs exhibited peaks with a relatively more negative shift, which is usually attributed to the stronger interaction of  $Ag^+$  with their CS backbones at the atomic level (Fig. 4C), indicating that the hydrophobic crowded nanosized microdomains formed by DCSs and the cooperative effect provided by the densely covered dendritic OEGs are favourable for strengthened complexation between the chitosan chains and metal ions.<sup>34,72</sup> The loading capacity of DCSs for  $AuCl_4^-$  increased from 68% at 32 °C to 99% at 75 °C (Fig. 4D), while the maximum loading amount of  $AuCl_4^-$  for  $TC_{xx}$  increased slightly with increasing metal ion concentration to 0.38 mg mg<sup>-1</sup> at 75 °C (Fig. 4E), over 10 times that previously reported.<sup>9</sup> This suggests that the dehydration and collapse of OEGs forced the CS backbones to be densely packed together and show cooperative effects in binding the metal ions. These results indicate that dendronization of CS with dendritic OEGs significantly furnishes CS advanced properties.<sup>73</sup>

#### 4.2 Switchable encapsulation for proteins

DCSs provide tunable crowding and hydrophobic microenvironment for manipulating interactions with proteins and modulating their bioactivity (Fig. 5A). The bioactivity of encapsulated proteins (myoglobin, Mb) within DCSs (named  $TC/Mb$ ) increased

continuously from 79% to 99% with the temperature increasing from 45 to 60 °C (above  $T_{cp}$ , Fig. 5B), which is over 2 times higher than that of other samples, including free Mb, PG1-proteins conjugates, PG1S-Mb, PG1 and a protein physical mixture (PG1/Mb, Fig. 5C). These are mainly owing to the suitable number of amino pendants in the CS backbones to provide the binding sites for complexation with proteins, and a proper amount of dendritic OEG pendants to provide sufficient shielding effects to form a hydrophobic microenvironment along the polymers, which prevents the proteins from undergoing strong solvation. The above results clearly indicate that the excellent features of DCSs inherited from CS have afforded these dendronized polymers with advantages for activity regulation of the biomacromolecules.<sup>2,59</sup>

#### 5. DCSs acting as nanoreactors for the fabrication of nanoparticles

Enhanced complexation of metal ions within DCSs encouraged us to investigate the possible *in situ* formation of nanoparticles within the DCSs, and a mild fabrication method for noble metal nanoparticles was developed. Complexed metal ions can be reduced to nanoparticles *in situ* with sufficient stability within 10 min when illuminated with visible light by using DCSs as the nanoreactor and reducing agent (Fig. 6A).

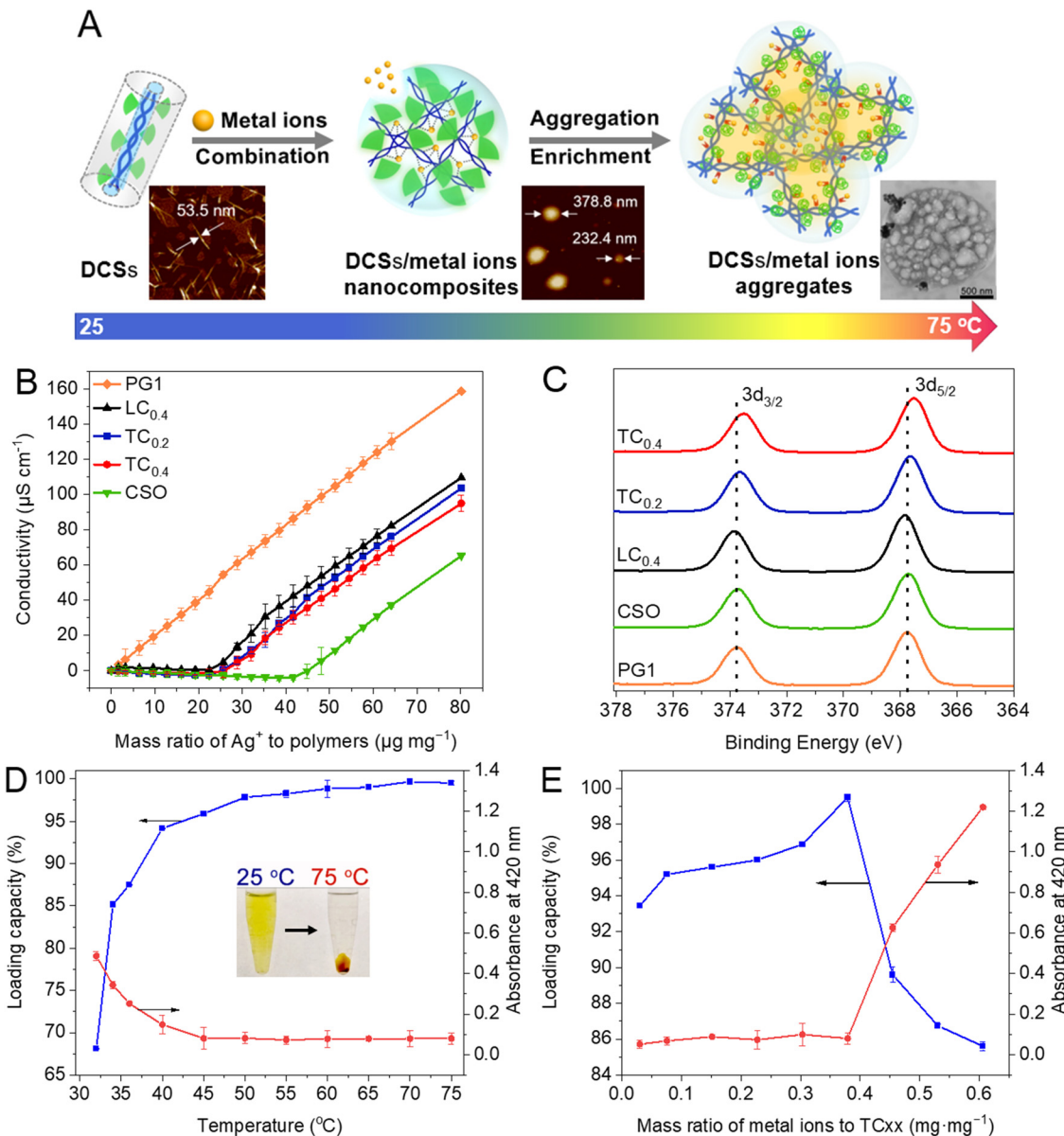


**Fig. 4** Switchable encapsulation for metal ions by DCSs. (A) Cartoon presentation of encapsulation for metal ions by DCSs. (B) Conductometric titration of  $\text{Ag}^+$  at 25 °C. (C) XPS spectra of  $\text{Ag}^+$  nanocomposites from different polymers. Loading capacity of DCSs for  $\text{AuCl}_4^-$  (D) at different temperatures (inset: photographs of their aqueous solutions at 25 and 75 °C, respectively), and (E) at 75 °C with different concentrations of  $\text{AuCl}_4^-$  and absorbance (at 420 nm) of their corresponding solutions, after being kept in the dark for 15 min. Reproduced from ref. 34 and 72 with permission from American Chemical Society, copyright 2022.

Moreover, composite metal nanoparticles, such as  $\text{Au}@\text{AgNPs}$  with different compositions (named **AuAg**) can be obtained simply by changing the feed ratios of metal ions through this methodology (Fig. 6B). The synthesized metal nanoparticles (AgNPs, Fig. 6C) were found to be spherical morphologies with average diameters around 5 nm, and single AgNPs showed clear interference fringe patterns demonstrating high crystallinity. Further, the formation rates ( $k_s$ ) of metal nanoparticles have been influenced by many facts, including structures and grafting coverage of dendritic OEGs and reaction temperature, with the main results including: (1) the  $k_s$  of DCSs is superior

to nature or linear-OEG modified CSs, because confined hydrophobic microenvironments provided by crowded OEG pendants enhance the complexation and reduction activity for metal ions (Fig. 6D); (2) DCSs with lower dendritic OEG coverage showed the highest  $k_s$ , indicating that the optimal grafting coverage of dendritic OEGs is beneficial; (3)  $k_s$  abruptly increased between 55 °C and 65 °C, due to the thermally-induced dehydration of dendritic OEGs from DCSs, which collapsed to form more hydrophobic microenvironments to accelerate the reduction<sup>74</sup> (Fig. 6E). These interesting observations indicate that cooperative

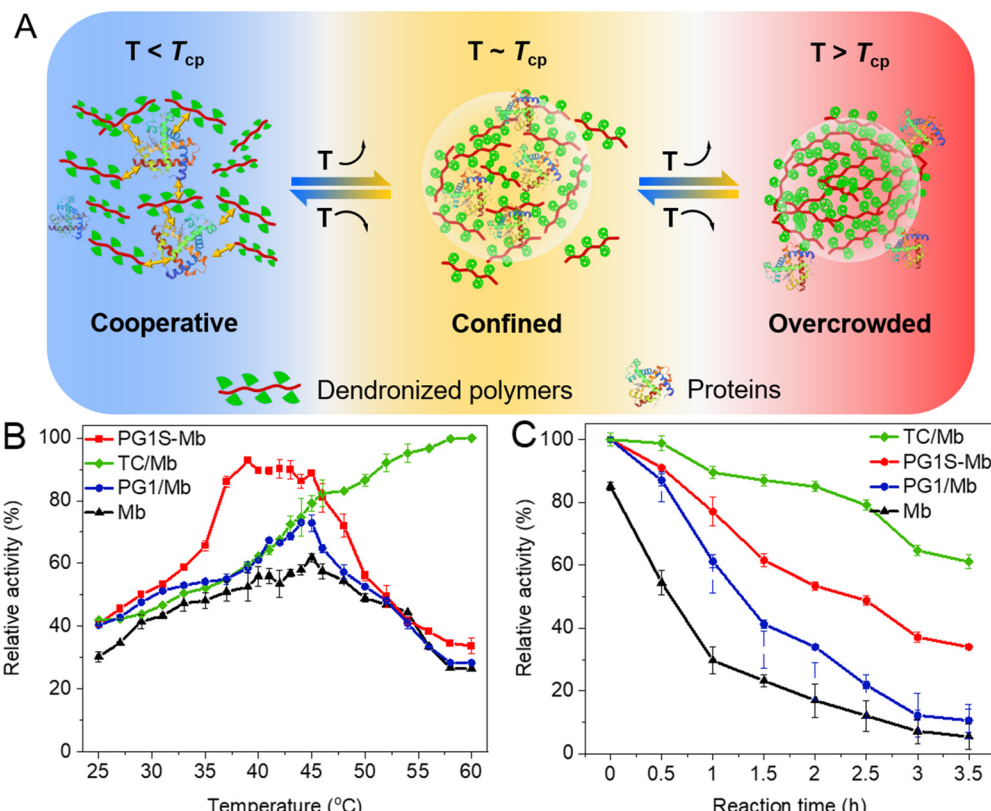


Fig. 5 Switchable encapsulation for proteins by DCSs. (A) Schematic representation for possible interaction modes between the dendronized polymers and proteins below, around, and above their  $T_{cps}$ . Quantitative relative activity of Mb from different samples at different temperatures (B), and after being kept at (C) 60 °C for different time intervals.<sup>59</sup>

combination of capacities from dendritic OEGs and CS backbones provides great potential for the DCSs to be used as nanoreactors in controllable fabrication of metal nanoparticles and simulating biomimetic mineralization.<sup>75,76</sup>

## 6. Higher level microconfinement from DCS hydrogels

One intriguing application for modified biomacromolecules is used for the fabrication of hydrogels through physical or chemical crosslinking.<sup>15,18,31</sup> These hydrogels exhibit prominent features, including similar characteristics of living tissues, biocompatibility, and biodegradation.<sup>23,77,78</sup> Recently, biomedical hydrogels with remarkable functions (stimuli-responsiveness, recognition, and activity regulation) have been continuously developed to modulate the migration or intermolecular association of guest molecules in a controlled manner, and have been used for switchable encapsulation of guests.<sup>31,71,76,79</sup>

### 6.1 Chemical and physical hydrogels from DCSs

DCSs carrying hydrophilic dendritic triethylene glycol pendants (TC<sub>xx</sub>) can form chemically crosslinked hydrogels through Schiff-base reaction, while DC<sub>xx</sub> carrying hydrophobic dendritic

diethylene glycol pendants formed highly transparent physical hydrogels with porous lamellar morphologies due to aggregation of the assembled fibers to form three-dimensional networks upon heating (Fig. 7A and B). These DCS hydrogels inherited featured biocompatibility from polysaccharides, and exhibited reversible sol-gel transition, injectable properties, and a remarkable self-healing ability (Fig. 7C). The thermogelling behavior and mechanical strengths of the hydrogels were mainly determined by the hydrophobicity and grafting ratio of the OEG dendrons, as well as the solid content of the DCSs. More importantly, the thermally induced aggregation feature of DCSs has a remarkable influence during their gelling process, which enhanced both Schiff-base reaction and the aggregation of polymer chains in the aqueous phase simultaneously, resulting in promoting crosslinking of the polymer networks for their gelation under physiological conditions and improvement of their mechanical properties. For the chemical hydrogels, a proper 3D microenvironment was provided for stem cell culture, and the embedded HMSCs and RNSCs could survive well and maintain their capability of differentiation (Fig. 7D). For the physical hydrogels, they can be injected at room temperature as a fluid, shape-fill irregular injuries and undergo *in situ* gelation *in vivo*, and can be used as hydrogel scaffolds and promote the growth of keratocytes and reduce the inflammatory response in a corneal tissue engineering test

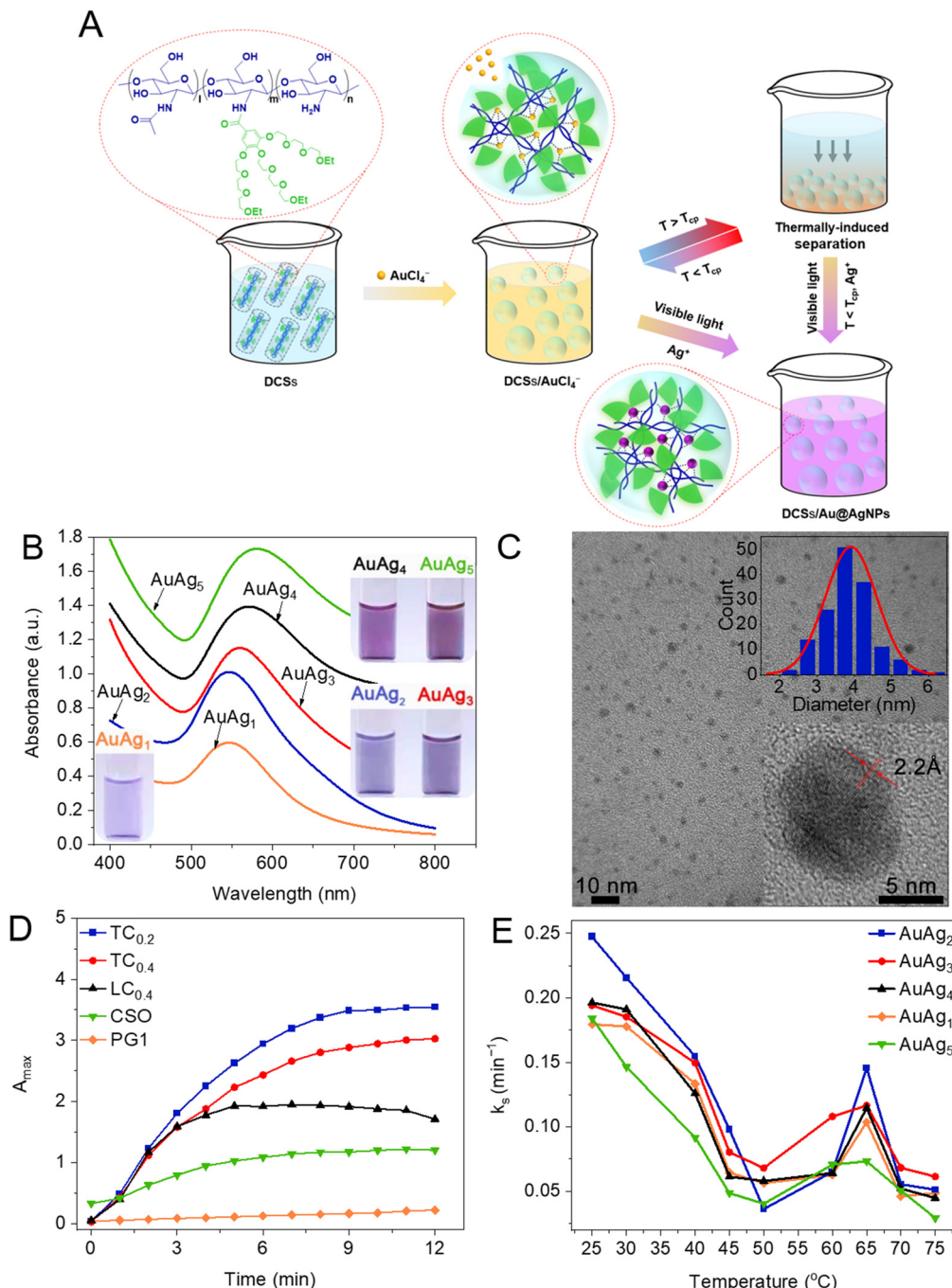


**Fig. 6** Fabrication of nanoparticles mediated by DCSs. (A) Schematic illustration of the preparation of Au@AgNPs mediated with DCSs and triggered by visible light. (B) UV-vis spectra of different Au@AgNPs (inset: photographs of the aqueous solutions). (C) TEM image of AgNPs synthesized from DCSs (insets: magnified region and particle size distribution). (D)  $A_{\max}$  (at 550 nm) of different Au@AgNPs after shining with visible light for every 1 min interval at 25 °C. (E) The  $k_s$  of Au@AgNPs synthesized by DCSs at different temperatures. Reproduced from ref. 34 and 72 with permission from American Chemical Society, copyright 2022.

using a rabbit model (Fig. 7E). Consequently, these DCS hydrogels have been considered as promising biomaterials to be used in diagnostics, therapeutics, and tissue engineering.<sup>36</sup>

## 6.2 Confinement of DCS hydrogels to proteins

Physical hydrogels with higher flowability were fabricated from DCSs with shorter CS main chains. These DCS hydrogels have a

reversible thermo-gelling property, allowing convenient and effective mixing with proteins at room temperature to prepare drug formulations and with controllable release capacity (Fig. 8A). With temperature increased from 40 to 65 °C (above  $T_{\text{gel}}$ ), the bioactivity of encapsulated horse-radish peroxidase (HRP) within DCS hydrogels increased from 72% to 99% for  $\text{DC}_{58}/\text{HRP}$  and 75% to 97% for  $\text{TC}_{84}/\text{HRP}$ , respectively, which

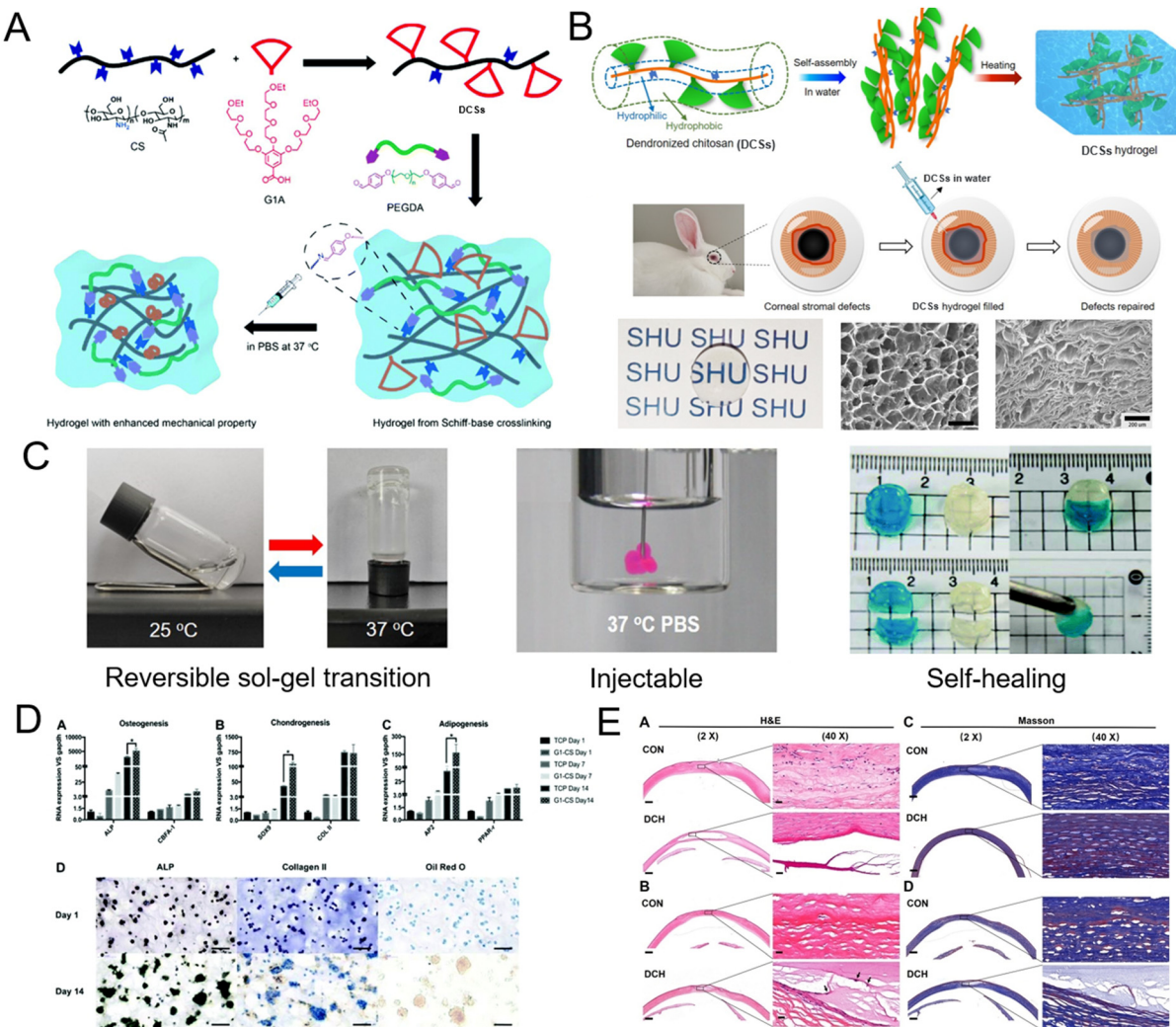


**Fig. 7** Schematic representation of the preparation of DCS hydrogels through (A) Schiff-base chemistry at room temperature and under physiological conditions,<sup>36</sup> and (B) thermally-induced gelation at physiological temperature and their application for corneal stromal defects. (C) Photographs of the reversible sol–gel transition, injection, and self-healing process, at 37 °C of DCS hydrogel. (D) Differentiation tendency of HMSCs after being cultured in DCS hydrogels. (E) Histological analysis after application of DCS hydrogels in a rabbit stromal defect model. Reproduced from ref. 35 with permission from American Chemical Society, copyright 2021.

makes a big contrast to the minor activity increase for the naked HRP (Fig. 8B). More importantly, the activity of proteins within DCS hydrogels remains higher than 50% after being kept at high temperature (65 °C) for 12 h, which appears better than that of linear DCS (Fig. 8C). This is mainly owing to the enhanced cooperative and shielding effect from OEG chains within the hydrogels, while providing a higher level confined microenvironment.<sup>71</sup> In addition, DCS hydrogels exhibited unique controllable release behavior, which could be conveniently achieved through their degradation mediated by degrading enzymes without losing the activities of enveloped proteins (Fig. 8D and E). Therefore, we believe that these DCS hydrogels with remarkable activity protection and controllable release properties may have promising applications for controlled delivery and tissue engineering.<sup>35,36,46,71,80</sup>

## 7. Conclusions and outlook

Through dendronization of CS with dendritic OEGs under environmentally friendly conditions, a series of DCSs were prepared with advanced properties, which form a unique pathway for convenient functionalization of polysaccharides. These water-soluble DCSs exhibit not only unique thermoresponsive behavior inherited from dendritic OEGs, but also biocompatibility and biodegradation inherited from polysaccharides. More importantly, densely packed dendritic OEGs around the CS backbones provided efficient cooperative interactions, affording an intriguing confined microenvironment to tune the complexation with metal ions and encapsulation of proteins, as well as to modulate the reduction of metal ions and formation of metal nanoparticles. Moreover, DCSs exhibit reversible thermo-gelling features to form highly transparent

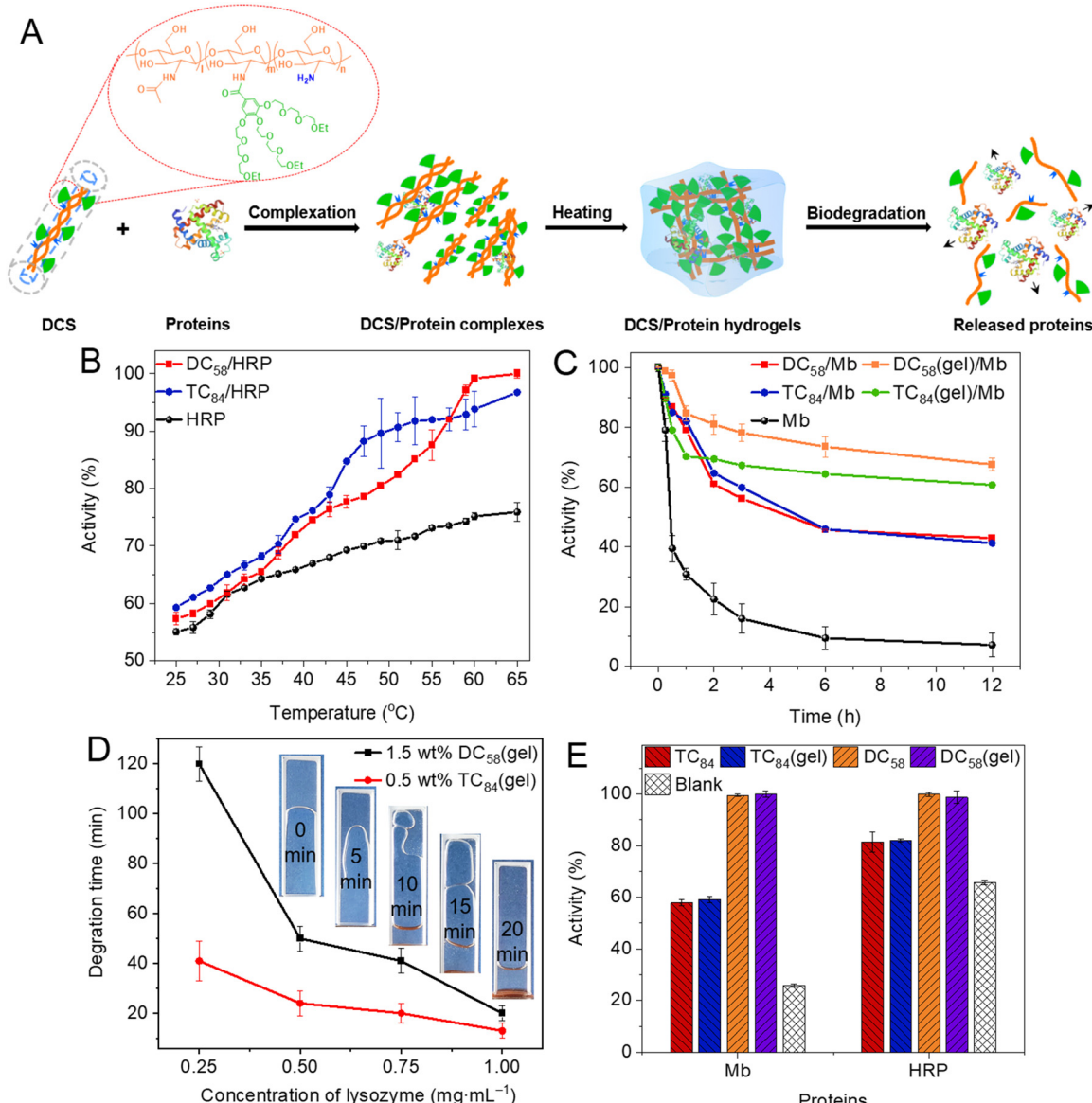


**Fig. 8** Regulation of activity and controlled release of proteins by DCS hydrogels. (A) Schematic illustration for formation of DCS hydrogels and applications in protein activity regulation. Quantitative protein activity from their physical mixture with DCSs and corresponding hydrogels (DCSs/proteins or DCSs(gel)/proteins) (B) at different temperatures after being kept for 30 min, and (C) after co-incubation with polymer solutions or hydrogels at 65 °C. (D) Degradation time of DCS hydrogels in the presence of different concentrations of lysozyme. (E) Quantitative protein activity for samples after co-incubation with lysozyme at different times. Reproduced from ref. 71 with permission from American Chemical Society, copyright 2022.

hydrogels with porous lamellar morphologies, while providing enhanced shielding and encapsulation to guests during the thermally-induced aggregation. In addition, DCS hydrogels provide higher level microconfinement to the encapsulated proteins because of the cooperative effects, and can control release of the guests through biodegradation of the DCSs.

Investigation on the fibrous morphology formation would be helpful to deeply understand why the DCSs form highly transparent hydrogels, and how to manipulate the mechanical properties of the formed materials. This will be important for further developing biomaterials based on these stimuli-responsive dendronized biomacromolecules. Further study

toward the fabrication of microgels with different sizes and morphologies from this class of DCSs may facilitate the establishment of bionic models and fabrication of promising smart materials such as for 3D cell culture based the environmental-friendly polymers, especially with higher level microconfinement through inter-molecularly cooperative interactions of the densely packed chains within the hydrogels.

The advances in understanding of microconfinement from these modified biodegradable biomacromolecules offer new research directions, which can be further explored by using dendritic OEGs with different branching densities, including 2-fold, 3-fold, 4-fold and 6-fold.<sup>12,53</sup> With different packing

densities of the OEG chains, crowding should be in different levels around the backbone of the biomacromolecules, which should be important in creating different levels of microconfinement for different application purposes, such as protection of proteins or nucleic acids, as well as drug delivery and drug targeting. We hope that the methodology developed in this perspective can provide some inspiration to functionalize other biomacromolecules, especially those carrying amino pendants, such as hyaluronic acid, gelatin or collagen.

## Author contributions

Y. Y. wrote the draft. W. L. and A. Z. revised the manuscript. All authors approved the final version.

## Conflicts of interest

There are no conflicts to declare.

## Acknowledgements

Financial support from the National Natural Science Foundation of China (No. 21971161), Shanghai Pujiang Program (No. 19PJ1403700) and Program for Professor of Special Appointment (Eastern Scholar TP2019039) at Shanghai Institutions of Higher Learning is acknowledged.

## References

- 1 R. J. Ellis, *Trends Biochem. Sci.*, 2001, **26**, 597–604.
- 2 G. Xu, K. Liu, B. Xu, Y. Yao, W. Li, J. Yan and A. Zhang, *Macromol. Rapid Commun.*, 2020, **41**, e2000325.
- 3 J. van den Berg, A. J. Boersma and B. Poolman, *Nat. Rev. Microbiol.*, 2017, **15**, 309–318.
- 4 D. Davidi, L. M. Longo, J. Jablonska, R. Milo and D. S. Tawfik, *Chem. Rev.*, 2018, **118**, 8786–8797.
- 5 F. Ma, X. Wu, A. Li, L. Xu, Y. An and L. Shi, *Angew. Chem., Int. Ed.*, 2021, **60**, 10865–10870.
- 6 A. Testa, M. Dindo, A. A. Rebane, B. Nasouri, R. W. Style, R. Golestanian, E. R. Dufresne and P. Laurino, *Nat. Commun.*, 2021, **12**, 6293.
- 7 C. J. Pedersen, *Science*, 1988, **241**, 536–540.
- 8 E. Słyk, T. Skóra and S. Kondrat, *Soft Matter*, 2022, **18**, 5366–5370.
- 9 R. Chapanian, D. H. Kwan, I. Constantinescu, F. A. Shaikh, N. A. A. Rossi, S. G. Withers and J. N. Kizhakkedathu, *Nat. Commun.*, 2014, **5**, 4683.
- 10 A. J. Boersma, I. S. Zuhorn and B. Poolman, *Nat. Methods*, 2015, **12**, 227–229.
- 11 J. Mandal and S. Ramakrishnan, *Langmuir*, 2015, **31**, 6035–6044.
- 12 J. Zhang, Y. Yao, Y. Zhang, D. Wu, W. Li, A. K. Whittaker and A. Zhang, *Macromolecules*, 2023, **56**, 3931–3944.
- 13 V. T. Ranganathan, S. Bazmi, S. Wallin, Y. Liu and A. Yethiraj, *Macromolecules*, 2022, **55**, 9103–9112.
- 14 Q. Zhang, L. Zhu, T. Hou, H. Chang, Q. Bai, J. Zhao and D. Liang, *Macromolecules*, 2019, **52**, 4251–4259.
- 15 J. Liao and H. Huang, *Biomacromolecules*, 2020, **21**, 2574–2594.
- 16 M. Darnell and D. J. Mooney, *Nat. Mater.*, 2017, **16**, 1178–1185.
- 17 K. Ren, H. Du, Z. Yang, Z. Tian, X. Zhang, W. Yang and J. Chen, *ACS Appl. Mater. Interfaces*, 2017, **9**, 10266–10275.
- 18 Y. Ou and M. Tian, *J. Mater. Chem. B*, 2021, **9**, 7955–7971.
- 19 S. P. Hoo, F. Sarvi, W. H. Li, P. P. Y. Chan and Z. Yue, *ACS Appl. Mater. Interfaces*, 2013, **5**, 5592–5600.
- 20 Y. Wu, D. Y. W. Ng, S. L. Kuan and T. Weil, *Biomater. Sci.*, 2015, **3**, 214–230.
- 21 J. Duan, X. Liang, Y. Cao, S. Wang and L. Zhang, *Macromolecules*, 2015, **48**, 2706–2714.
- 22 V. K. Thakur and M. K. Thakur, *ACS Sustainable Chem. Eng.*, 2014, **2**, 2637–2652.
- 23 K. Fukada, T. Tajima and M. Seyama, *ACS Appl. Mater. Interfaces*, 2021, **13**, 59006–59011.
- 24 A. Basu, K. R. Kunduru, E. Abtew and A. J. Domb, *Bioconjugate Chem.*, 2015, **26**, 1396–1412.
- 25 F. Liu, X. Liu, F. Chen and Q. Fu, *Prog. Polym. Sci.*, 2021, **123**, 101472.
- 26 S. Mukherjee, S. Jana, S. Khawas, J. Kicuntod, M. Marschall, B. Ray and S. Ray, *Carbohydr. Polym.*, 2022, **289**, 119299.
- 27 Y. C. E. Li, *ACS Biomater. Sci. Eng.*, 2019, **5**, 2079–2092.
- 28 L. Barbier, M. Protat, P. Pipart, A. Marcellan, Y. Tran and D. Hourdet, *Carbohydr. Polym.*, 2023, **310**, 120715.
- 29 D. Hua, J. Jiang, L. Kuang, J. Jiang, W. Zheng and H. Liang, *Macromolecules*, 2011, **44**, 1298–1302.
- 30 C. Pitakchatwong and S. Chirachanchai, *ACS Appl. Mater. Interfaces*, 2017, **9**, 10398–10407.
- 31 T. Vermonden, R. Censi and W. E. Hennink, *Chem. Rev.*, 2012, **112**, 2853–2888.
- 32 C. G. Palivan, R. Goers, A. Najar, X. Zhang, A. Car and W. Meier, *Chem. Soc. Rev.*, 2016, **45**, 377–411.
- 33 L. Bai, L. Liu, M. Esquivel, B. L. Tardy, S. Huan, X. Niu, S. Liu, G. Yang, Y. Fan and O. J. Rojas, *Chem. Rev.*, 2022, **122**, 11604–11674.
- 34 Y. Yao, K. Zhang, J. Chen, W. Li and A. Zhang, *ACS Sustainable Chem. Eng.*, 2022, **10**, 8265–8274.
- 35 L. Feng, R. Liu, X. Zhang, J. Li, L. Zhu, Z. Li, W. Li and A. Zhang, *ACS Appl. Mater. Interfaces*, 2021, **13**, 49369–49379.
- 36 X. Zhang, L. Cheng, L. Feng, Y. Peng, Z. Zhou, G. Yin, W. Li and A. Zhang, *Polym. Chem.*, 2019, **10**, 2305–2315.
- 37 J. Zeng, Y. He, S. Li and Y. Wang, *Biomacromolecules*, 2012, **13**, 1–11.
- 38 C. Federer, M. Kurpiers and A. Bernkop-Schnürch, *Biomacromolecules*, 2021, **22**, 24–56.
- 39 J. Deng, Y. Zhou, B. Xu, K. Mai, Y. Deng and L. Zhang, *Biomacromolecules*, 2011, **12**, 642–649.
- 40 V. G. Muir and J. A. Burdick, *Chem. Rev.*, 2021, **121**, 10908–10949.
- 41 R. L. G. Lecaros, Z. C. Syu, Y. H. Chiao, S. R. Wickramasinghe, Y. L. Ji, Q. F. An, W. S. Hung, C. C. Hu, K. R. Lee and J. Y. Lai, *Environ. Sci. Technol.*, 2016, **50**, 11935–11942.

42 X. Li, Y. Wang, C. Feng, H. Chen and Y. Gao, *Biomacromolecules*, 2022, **23**, 2197–2218.

43 L. Juan, S. Lin, C. Wong, U. S. Jeng, C. Huang and S. Hsu, *ACS Appl. Mater. Interfaces*, 2022, **14**, 36353–36365.

44 G. Huang, F. Li, X. Zhao, Y. Ma, Y. Li, M. Lin, G. Jin, T. J. Lu, G. M. Genin and F. Xu, *Chem. Rev.*, 2017, **117**, 12764–12850.

45 Z. Luo, K. Xue, X. Zhang, J. Y. C. Lim, X. Lai, D. J. Young, Z. X. Zhang, Y. L. Wu and X. J. Loh, *Biomater. Sci.*, 2020, **8**, 1364–1379.

46 M. Kim, Y. Ahn, K. Lee, W. Jung and C. Cha, *Carbohydr. Polym.*, 2020, **229**, 115538.

47 Y. Ding, X. Zhang, B. Xu and W. Li, *Polym. Chem.*, 2022, **13**, 2813–2821.

48 Y. Ding, X. Zhang, W. Li and A. Zhang, *Molecules*, 2022, **27**, 6096.

49 E. M. Pelegri-O'Day and H. D. Maynard, *Acc. Chem. Res.*, 2016, **49**, 1777–1785.

50 O. Harel and M. Jbara, *Angew. Chem., Int. Ed.*, 2023, **62**, e202217716.

51 J. Cao, O. T. Zaremba, Q. Lei, E. Ploetz, S. Wuttke and W. Zhu, *ACS Nano*, 2021, **15**, 3900–3926.

52 J. F. G. A. Jansen, E. M. M. de Brabander-van den Berg and E. W. Meijer, *Science*, 1994, **266**, 1226–1229.

53 G. Xu, J. Zhang, R. Jia, W. Li and A. Zhang, *Macromolecules*, 2022, **55**, 630–642.

54 M. J. N. Junk, W. Li, A. D. Schlüter, G. Wegner, H. W. Spiess, A. Zhang and D. Hinderberger, *Angew. Chem., Int. Ed.*, 2010, **49**, 5683–5687.

55 D. Luong, P. Kesharwani, R. Deshmukh, M. C. I. Mohd Amin, U. Gupta, K. Greish and A. K. Iyer, *Acta Biomater.*, 2016, **43**, 14–29.

56 G. N. Rimondino, M. C. Strumia and M. Martinelli, *ACS Sustainable Chem. Eng.*, 2014, **2**, 2582–2587.

57 M. A. Kostiainen, O. Kasyutich, J. J. Cornelissen and R. J. Nolte, *Nat. Chem.*, 2010, **2**, 394–399.

58 J. Yan, X. Zhang, W. Li, X. Zhang, K. Liu, P. Wu and A. Zhang, *Soft Matter*, 2012, **8**, 6371–6377.

59 Y. Yao, J. Yang, W. Li and A. Zhang, *Polym. Chem.*, 2022, **13**, 5404–5411.

60 Y. Yao, J. Wu, S. Cao, B. Xu, J. Yan, D. Wu, W. Li and A. Zhang, *Chin. J. Polym. Sci.*, 2020, **38**, 1164–1170.

61 M. Recillas, L. L. Silva, C. Peniche, F. M. Goycoolea, M. Rinaudo and W. M. Argüelles-Monal, *Biomacromolecules*, 2009, **10**, 1633–1641.

62 S. Sun, W. Liu, N. Cheng, B. Zhang, Z. Cao, K. Yao, D. Liang, A. Zuo, G. Guo and J. Zhang, *Bioconjugate Chem.*, 2005, **16**, 972–980.

63 S. M. Cheal, M. Patel, G. Yang, D. Veach, H. Xu, H. Guo, P. B. Zanzonico, D. B. Axworthy, N. K. V. Cheung, O. Ouerfelli and S. M. Larson, *Bioconjugate Chem.*, 2020, **31**, 501–506.

64 X. Zhao, H. Sun, X. Zhang, J. Ren, F. Shao, K. Liu, W. Li and A. Zhang, *Polymer*, 2016, **99**, 281–291.

65 J. Yan, K. Liu, W. Li, H. Shi and A. Zhang, *Macromolecules*, 2016, **49**, 510–517.

66 A. Qian, K. Liu, P. Chen, Y. Yao, J. Yan, W. Li, X. Zhang and A. Zhang, *Macromolecules*, 2019, **52**, 3454–3461.

67 J. Yan, W. Li and A. Zhang, *Chem. Commun.*, 2014, **50**, 12221–12233.

68 R. Lopez-Blanco, M. Fernandez-Villamarín, S. Jatunov, R. Novoa-Carballal and E. Fernandez-Megia, *Polym. Chem.*, 2019, **10**, 4709–4717.

69 M. C. García, A. A. Aldana, L. I. Tártara, F. Alovero, M. C. Strumia, R. H. Manzo, M. Martinelli and A. F. Jimenez-Kairuz, *Carbohydr. Polym.*, 2017, **175**, 75–86.

70 W. Wang, X. Zhang, Z. Li, D. Pan, H. Zhu, Z. Gu, J. Chen, H. Zhang, Q. Gong and K. Luo, *Carbohydr. Polym.*, 2021, **267**, 118160.

71 Y. Yao, S. Cao, Q. Yang, A. Zhang and W. Li, *ACS Appl. Bio. Mater.*, 2022, **5**, 5377–5385.

72 Y. Yao, S. Cao, X. Zhang, J. Yan, W. Li, A. Whittaker and A. Zhang, *ACS Appl. Nano Mater.*, 2022, **5**, 4350–4359.

73 W. Du, Z. Zhao and X. Zhang, *Carbohydr. Polym.*, 2022, **285**, 119232.

74 M. Naodovic and H. Yamamoto, *Chem. Rev.*, 2008, **108**, 3132–3148.

75 S. J. Omelon and M. D. Grynpas, *Chem. Rev.*, 2008, **108**, 4694–4715.

76 X. Feng, J. Liu, G. Xu, X. Zhang, X. Su, W. Li and A. Zhang, *J. Mater. Chem. B*, 2018, **6**, 1903–1911.

77 Q. Liu, G. Nian, C. Yang, S. Qu and Z. Suo, *Nat. Commun.*, 2018, **9**, 846.

78 S. Correa, A. K. Grosskopf, H. Lopez Hernandez, D. Chan, A. C. Yu, L. M. Stapleton and E. A. Appel, *Chem. Rev.*, 2021, **121**, 11385–11457.

79 C. Zhou, M. A. Abdel-Rahman, W. Li, K. Liu and A. Zhang, *Chin. Chem. Lett.*, 2017, **28**, 832–838.

80 S. S. Liow, Q. Dou, D. Kai, A. A. Karim, K. Zhang, F. Xu and X. J. Loh, *ACS Biomater. Sci. Eng.*, 2016, **2**, 295–316.